Computer Methods and Programs in Biomedicine 178 (2019) 41–46

Contents lists available at ScienceDirect

Computer Methods and Programs in Biomedicine

journal homepage: www.elsevier.com/locate/cmpb

Design of smart EEG cap

Bor-Shing Lin[a], Yao-Kuang Huang[b], Bor-Shyh Lin[c,d,*]

[a] Department of Computer Science and Information Engineering, National Taipei University, New Taipei City, 23741 Taiwan
[b] Division of Cardiovascular Surgery, Chia-Yi Chang Gung Memorial Hospital, Chiayi, Taiwan
[c] Institute of Imaging and Biomedical Photonics, National Chiao Tung University, Tainan, 71150 Taiwan
[d] Department of Medical Research, Chimei Medical Center, Tainan, Taiwan

ARTICLE INFO

Article history:
Received 10 March 2019
Revised 27 May 2019
Accepted 10 June 2019

Keywords:
Brain machine interface
EEG cap
Spatial filtering circuit
Dry active electrode

ABSTRACT

Background and Objective: Brain machine interface (BMI) is a system which communicates the brain with the external machines. In general, an electroencephalograph (EEG) machine has to be used to monitor multi-channel brain responses to improve the BMI performance. However, the bulky size of the EEG machine and applying conductive gels in EEG electrodes also cause the inconvenience of daily life applications. How to select the relevant EEG channel and remove irrelevant channels is important and useful for the development of BMIs.

Methods: In this research, a smart EEG cap was proposed to improve the above issues. Different from the conventional EEG machine, the proposed smart EEG cap contain a spatial filtering circuit to enhance EEG features in local area, and it could also select the relevant EEG channel automatically. Moreover, the novel dry active electrodes were also designed to acquire EEG without conductive gels in the hairy skin of the head, to improve the convenience in use.

Results: Finally, the proposed smart EEG cap was applied in motion imagery-based BMI and several experiments were tested to valid the system performance. The proposed smart EEG cap could effectively enhance EEG features and select relevant EEG channel, and the information transfer rate of BMI was about 6.06 bits/min.

Conclusions: The proposed smart EEG cap has advantages of measuring EEG without conductive gels and wireless transmission to effectively improve the convenience of use, and reduce the limitation of activity in daily life. In the future, it might be widely applied in other BMI applications.

1. Introduction

Electroencephalograph (EEG)-based brain machine interface is a system which can translate the mental tasks of the user into a command to communicate with the external device without using muscle [1,2]. Most of BMIs require many EEG channels to acquire EEG signals from multiple sites on the scalp skin to provide a good performance. Before measuring multi-channel brain responses, a prolonged preparation time is required and it directly affects the convenience in use. Moreover, these EEG channels may contain many irrelevant signals, Therefore, for the development of brain machine interfaces (BMIs), selecting the optimal subset of the EEG channels to replace the use of all EEG channels is an important issue.

Several approaches in previous studies have been designed to extract the optimal subset of the EEG channels to improve the BMI performance. In order to remove the noisy and irrelevant channels, the sparse common spatial pattern (SCSP) method proposed by Arvaneh et al. was used to retain the least EEG channels and provide a good accuracy of classification which is similar to that obtained by using all EEG channels [3]. Lal et al. used the technique of support vector machines (SVM) to the art feature selection methods, and applied it in the problem of channel selection [4]. Here, EEG features derived from autoregressive (AR) models were used to eliminate the EEG channels which least-contributed in the accuracy of classification. Lan et al. designed a mutual-information-based dimensionality reduction method to select EEG channels [5]. The mutual information between the class labels and the EEG channels were used to determine the channel selection. By selecting the meaningful EEG channels and removing irrelevant EEG channels, the performance of BMIs could be improved [3]. Moreover, reducing the number of the required EEG channels could improve the convenience of use, and the computational complexity of BMIs could also be reduced straightforwardly. However,

* Corresponding author at: Institute of Imaging and Biomedical Photonics, National Chiao Tung University, No.301, Gaotie 3rd Rd., Guiren Dist., Tainan, 71150 Taiwan.
E-mail address: borshyhlin@nctu.edu.tw (B.-S. Lin).

https://doi.org/10.1016/j.cmpb.2019.06.009
0169-2607/

the above BMIs still required many EEG electrodes with conductive gels and the conventional EEG machine to acquire multi-channel brain responses, and these EEG signals would be sent to the back-end BMI platform to select the optimal subset of the EEG channels. It also reduces the practicability of BMIs and increases the limitation of BMI applications.

Based on the concept of selecting the optimal subset of the EEG channels, a smart EEG cap was proposed in this study. Here, novel dry active electrodes were designed to acquire EEG without conductive gels from the hairy site of the head. Moreover, the impedance test circuit for electrode-skin interface impedance was designed in the smart EEG cap to ensure each dry active electrode contacting with the skin well. Different from other BMIs that have to acquire and transmit multi EEG channels to the back-end BMI platform to select the optimal subset of the EEG channels, the proposed smart EEG cap could select the relevant EEG channels directly after acquiring EEG signals. It also contains a spatial filtering circuit to enhance the specific EEG features within a local spatial distribution. Finally, the proposed smart EEG cap was applied in the application of motion-imagery-based BMIs to improve the issue of the relevant EEG channels related to motion imagery is varied from subject to subject.

2. System architecture and design

The proposed smart EEG cap, as illustrated in Fig. 1(a) and (b), mainly contained a mechanical design, dry active electrodes, a wireless bio-potential acquisition module. The mechanical design of the smart EEG cap with the dry active electrodes were designed to acquire EEG signal without conductive gels in the hairy head skin. The wireless bio-potential acquisition module was designed to amplify the acquired bio-potential signal, perform the function of spatial filtering and selecting the relevant EEG channel, and transmit the selected-channel EEG signals to the BMI platform via Bluetooth. Finally, the BMI platform would receive the selected-channel EEG signals and perform the function of motion-imagery BMIs. In the BMI platform, a BMI program was also designed to provide several functions, including impedance testing of electrode-skin interface and detecting motion imagery event.

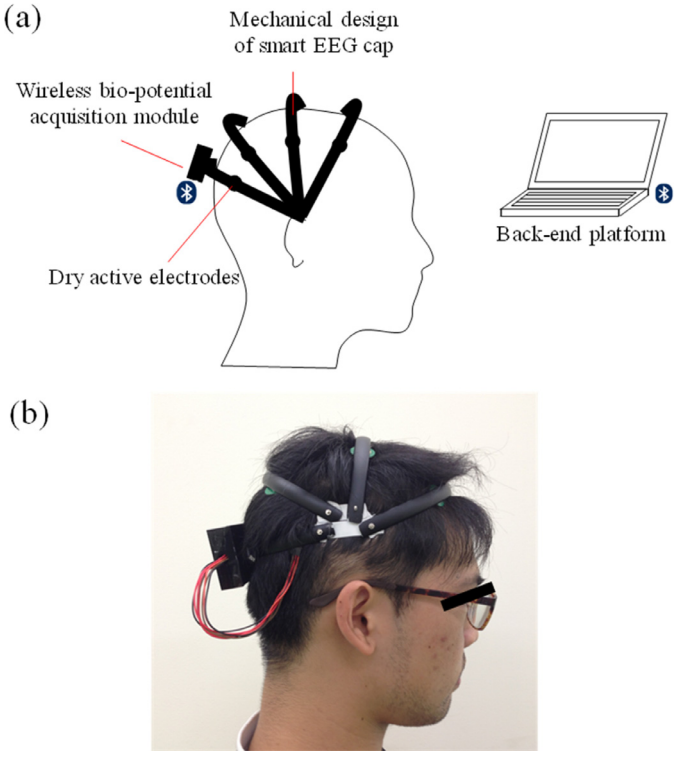

Fig. 1. (a) System architecture and (b) photograph of proposed smart EEG cap.

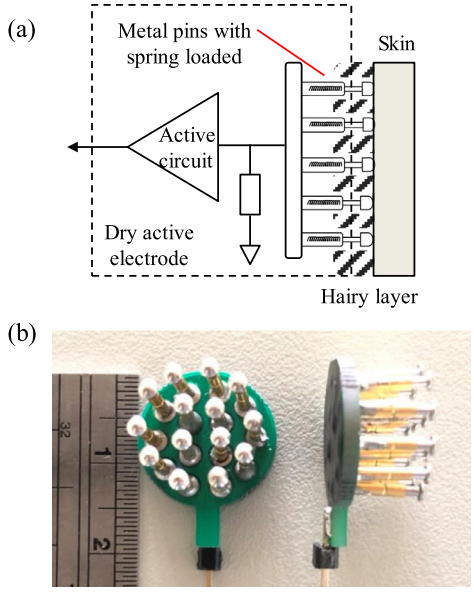

Fig. 2. (a) Structure illustration and (b) photograph of designed dry active electrode.

2.1. Mechanical design of smart EEG cap with dry active electrodes

Fig. 2(a) and (b) showed the basic structure and photograph of the designed dry active electrode respectively, and it was implemented to acquire bio-potential without conductive gels, in the hairy head skin. It mainly contains the active circuit part and the metal electrode part. The metal electrode part, made of copper, was coated with Ag, and was connected with many metal pins with spring loaded. These metal pins could easily pass through the head hair to touch the head skin well, and the spring in the metal pins allow it contacting with the irregular skin well. For the active circuit part, its input impedance was ultra-high to avoid the distortion or attenuation of the acquired bio-potential. Moreover, the wearable device design could also provide a suitable pressure and ensure a good and stable contact status between the skin and the electrode. For the mechanical design, it mainly consisted of four flexible plastic strips similar to Alice band. The dry active electrodes were embedded into the plastic strips. These dry active electrodes were placed on O1, O2, P3, P4, C3, C4, F3, and F4 of the international 10–20 EEG system respectively.

2.2. Wireless bio-potential acquisition module

The designed wireless bio-potential acquisition module, as illustrated in Fig. 3(a), mainly contained front-end bio-amplifier circuits, an impedance test circuit for electrode-skin interface, a common average reference (CAR) spatial filtering circuit, a microprocessor unit, and a Bluetooth module. The dimension of the wireless bio-potential acquisition module was about $8.3 \times 5.2 \times 2\,cm^3$. It could operate with 3.5-V DC power supply, and its current consumption was about 28 mA. By using a 350 mAh Li-ion battery, it operation time was over 12 h. The impedance test circuit, which provided a 10 Hz signal source to pass through the electrode-skin interface to evaluate its impedance [6], was designed to check the electrode-skin contact status. The whole

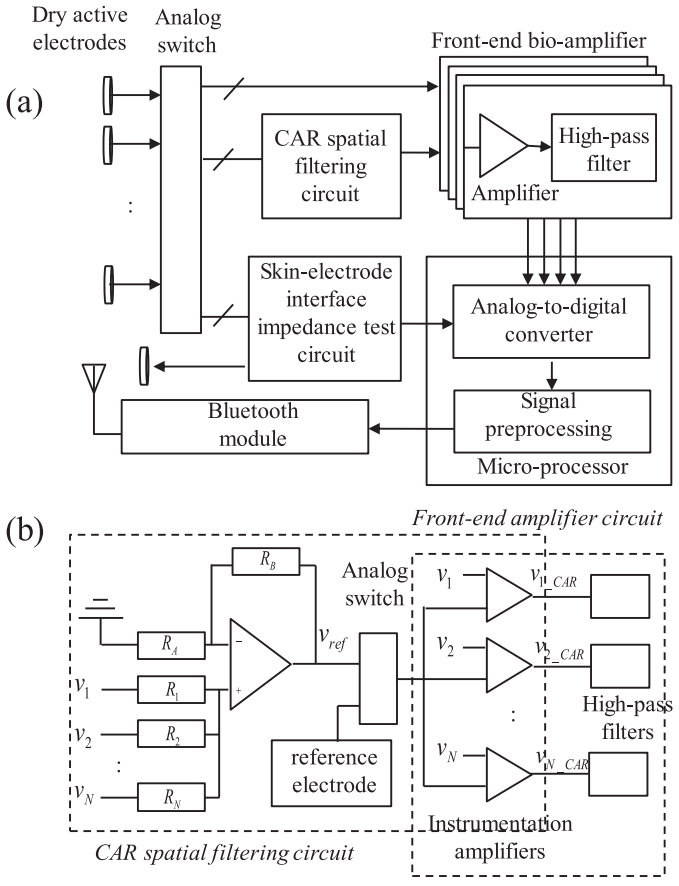

Fig. 3. Block diagrams of (a) wireless bio-potential acquisition module, and (b) CAR spatial filtering circuit.

gain of the bio-amplifier circuit was set to 10,000, and it was designed to amplify the acquired bio-potential signal.

In 1997, McFarland et al. investigated the effect of selecting different spatial filter, including two types of Laplacian derivations, common average reference, and conventional ear reference, on the performance of EEG-based BMIs, and indicated that the Large Laplacian derivations spatial filter and CAR spatial filter could provide the better BMI performance [7]. In this study, the common average reference spatial filtering circuit was designed for the enhancement of the specific EEG feature within a local spatial distribution. Let an EEG system contain N channels and $v_i(t)$ denote the raw signal of the i th EEG channel at iteration t, and then the EEG signal processed by the CAR spatial filter can be expressed by

$$v_{i,CAR}(t) = v_i(t) - \frac{1}{N}\sum_{n=1}^{N} v_n(t) \quad (1)$$

where $v_{i,CAR}(t)$ denotes i th channel filtered EEG signal at iteration t. Fig. 3(b) illustrated the schematic circuit of the CAR spatial filtering circuit. In this circuit, an adder was used to sum up the N-channel EEG signals. The resistances R_A and R_B in the adder were used to adjust the gain of the adder, and the resistances R_1,R_2,..., R_N were used to determine the weight of input raw EEG signals. The instrumentation amplifiers in the front-end bio-amplifier circuits were used as subtractors to subtract the average of the N-channel raw EEG signals to obtain the filtered EEG signals $v_{i,CAR}(t)$, $i = 1, 2, \ldots, N$. The microprocessor was designed to digitize bio-potential signals with 512 Hz sampling rate, and perform the function of selecting the relevant EEG channels. Next, the selected-channel EEG signals would be sent to the Bluetooth module, to transmit to the host system wirelessly.

3. Methods

The hand motion or motion imagery can reflect on β rhythm (13–30 Hz) and μ (8 Hz–13 Hz), acquired from the sensory-motor cortex. In 1977, the phenomenon of event-related desynchronization (ERD) and event-related synchronization (ERS) was first introduced [8,9]. They found that the decrease of EEG power in β rhythm and μ rhythm measured from the sensory-motor cortex occurred under the motion imagery of the hand, and the increase of EEG power in β rhythm and μ rhythm occurred after motion imagery. According to the above phenomenon, the criterion of selecting the optimal subset of the EEG channels was designed in this study.

For the stage of selecting the relevant EEG channels, the BMI program would show the icons of the stop mark, left arrow or right arrow to instruct the user to do nothing, right hand or left hand motion imagery respectively. The whole test procedure of selecting the relevant EEG channels would perform three right hand and left hand motion imagery actions sequentially, and the period of each motion imagery was about 10 s. In each cycle, the user would be instructed to relax within the first 4 s, and perform the motion imagery within the last 6 s.

In order to extract the features related to the motion imagery, the normalization of ERD [2, 10], as illustrated in Fig. 4(a), could be calculated as followings.

$$ERD(k) = \frac{P_{ERD}(k) - P_{baseline}}{P_{baseline}} \times 100\ (\%) \quad (2)$$

where $P_{baseline}$ denotes the averaged power of the first 4 s μ rhythm EEG. $P_{ERD}(k)$ denotes the k-th averaged power of the 2 s μ rhythm EEG with the overlap of 1 s EEG. Finally, the channel, that provided

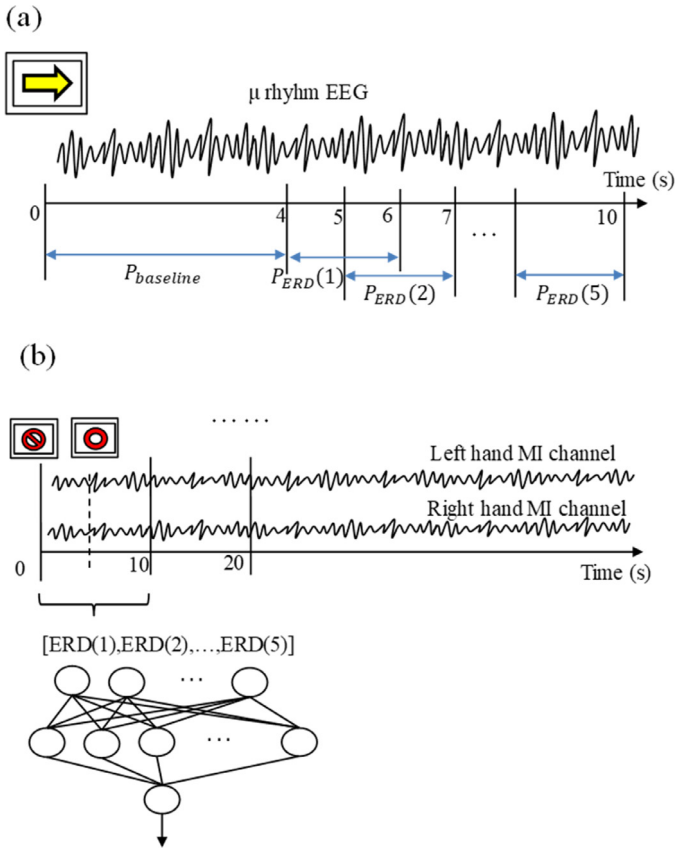

Fig. 4. Illustration of (a) extracting ERD quantification from μ rhythm EEG, and (b) motion-imagery detection.

the minimum of the ERD normalization *ERD*(1), would be selected as the relevant channel related to right hand or left hand motion imagery.

For the design of motion-imagery-based BMI, the ERD normalization vector [*ERD*(1), *ERD*(2), ..., *ERD*(5)] extracted from the selected-channel EEG was used as the EEG feature of detecting motion imagery. Here, a neural network with 64 hidden neurons was used to training the model of right hand and left hand motion imagery. Here, radial basis function neural network, which can provide a multi-dimensional approximation, and contains the advantages of simpler structure, and fast training procedure, was used in this study [11]. In the beginning, the BMI program would periodically show two cues to instruct the user. The first cue would instruct the user to relax for 4 s, and the second cue would instruct the user to do motion imagery for 6 s. After each cycle, the ERD normalization vectors extracted from the two selected channels related to right hand or left hand motion imagery would be calculated, and were used as the input of the neural network. If the ERD normalization of the selected channels was lower than the given threshold, the channel containing the minimum ERD normalization would be recognized as the event of motion imagery. If all ERD normalizations of the selected channels were higher than the given threshold, it would be recognized as the do-no-thinking state. The whole procedure of motion-imagery detection was illustrated in Fig. 4(b).

4. Experimental results

4.1. Performance of smart EEG cap on EEG enhancement and selecting channel

In this section, the selected EEG channels and ERD normalization obtained by the proposed smart EEG cap when the participants performed the right/left hand motion imagery were first investigated. The selected EEG channels and their ERD normalization under the right/left hand motion imagery were showed in Fig. 5(a) and (b) respectively. A total of 25 subjects (23 men and 2 women, mean age: 25.73 ± 2.1 years) attended this experiment. For the right hand motion imagery, the selected EEG channels could be F3, C3, and P3. The selected EEG channels for the left hand motion imagery could be F4, C4, and P4. Here, most of the selected channels under right/left hand motion imagery were at the locations of C3 and C4 respectively. The range of ERD normalization for the right/left hand motion imageries were about from −50% to −20%.

Next, the performance of the proposed smart EEG cap on enhancing EEG within a local spatial distribution was first tested. Here, EEG signals acquired from the locations of C3 and C4 in 10–20 EEG system when performing motion imagery, were used for test. The definition of the performance on enhancing ERD feature was the difference between the normalization ERD values of *ERD*(1) with and without the CAR spatial filtering circuit. The experimental results showed the averaged performance of enhancing ERD feature by using the CAR spatial filtering circuit was about 17.33 ± 11.93%. Therefore, EEG within a local spatial distribution could exactly be enhanced by the proposed smart EEG cap.

4.2. Performance of smart EEG cap applied in motion-imagery BMI

The BMI performance of the proposed smart EEG cap was investigated in this section. In the beginning of this experiment, a stop mark was presented to instruct the user to do nothing for 4 s. Next, a randomly selected arrow mark was presented to instruct the user to do right hand or left hand motion imagery. The period of each hand motion imagery test was about 10 s. A total of 10 subjects (10 males, mean age: 24.78 ± 1.5 years) attended this experiment, and all subjects were simply trained for half of an hour. Before evaluating the performance on detecting motion imagery, the binary classification test parameters have to be first defined: (i) True positive indicates the right/left hand motion imagery was correctly recognized as an action of right/left hand motion imagery, (ii) True negative indicates the state of doing nothing correctly recognized as an idle state, (iii) False positive indicates the state of doing nothing was incorrectly recognized as an action of right/left hand motion imagery, and (iv) False negative indicates the right/left hand motion imagery was incorrectly recognized as an action of left/right hand motion imagery or an idle state. Here, the performance of the proposed system on recognizing motion imagery was evaluated by F-measure, and it can be calculated from sensitivity and positive predictive value (PPV)

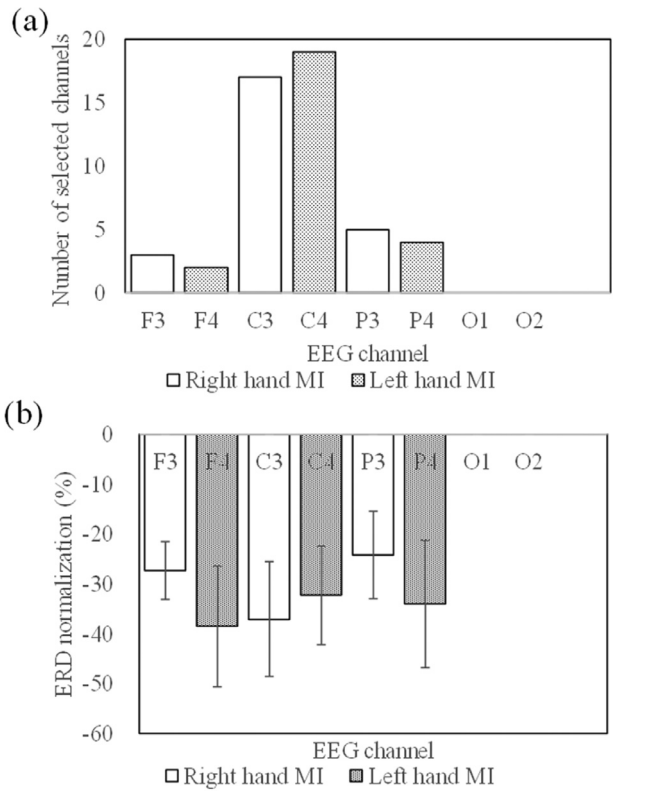

Fig. 5. (a) Selected EEG channels and (b) ERD normalization obtained by proposed smart EEG cap under right hand and left hand motion imageries.

The performance on recognizing left and right hand motion imageries by using the proposed smart EEG cap were listed in Fig. 6. It showed that the averaged F-measure values for detecting motion imagery was about 74.64 ± 4.88%. The averaged PPV and sensitivity for detecting motion imagery were 73.44 ± 7.25% and 76.39 ± 5.92% respectively. The accuracy of recognizing motion-imagery event was 73.19 ± 5.20%. Next, the information transfer rate (ITR) [12, 13] was evaluated, and the definition of the information transfer rate was given by

$$B = \log_2 N + P\log_2 P + (1-P)\log_2[(1-P)(N-1)] \quad (3)$$

where B is the information transfer rate, P is the accuracy of recognizing motion imagery, and N is the number of mental processes. Then, the definition of bit rate is given by (bits/ symbol) × (symbols/min). In this system, N was set to 3, including the state of doing nothing and the right/left hand motion imagery. In the proposed system, its information transfer rate was about 1.01 bits per trial (bit rate = 6.06 bits/min).

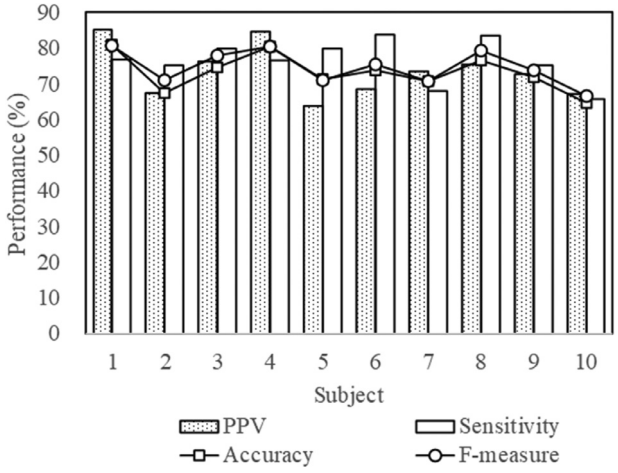

Fig. 6. PPV, sensitivity, F-measure, and accuracy of motion-imagery detection by using proposed smart EEG cap.

5. Discussions

In the proposed smart EEG cap, dry active electrodes were designed and applied in EEG measurement. The design of the pin-shaped electrode with spring loaded can easily separate the head hair and contact with the irregular skin well, and the part of the active circuit can reduce the signal attenuation and phase distortion due to its low input current and ultra-high input impedance [14]. The wearable mechanical design also provided a slight pressure to ensure a good and stable contact status between the skin and the electrode to acquire a good EEG signal quality. Moreover, it also could help the user easily wearing to improve the convenience in daily life use. The CAR spatial filtering circuit with 8 EEG channels (O1, O2, P3, P4, C3, C4, F3, and F4) was also designed and implemented in this smart EEG cap and its performance of enhancing ERD feature was also good. Mohammed J. Alhaddad indicated that the performance of CAR spatial filter outperformed that of the other re-references techniques [15]. They also indicated that the performances of the CAR spatial filter with 8, 16, and 32 channels were similar, and the accuracy of BMI obviously became poorer when reducing the EEG channel number to 4 channels. S.C. Ng and P. Raveendran used 26 EEG channels around the motor cortex region to perform the CAR spatial filter. They indicated that it cannot provide a good performance of enhancing EEG feature related to motion imagery when all of the EEG channels were around the motor cortex region [16]. The EEG channels selected near the motor-sensory cortex might cause that a large proportion of specific EEG related to motion imagery was merged into the common mode signal, and this also reduced the efficiency of enhancing specific EEG features within a local spatial distribution. The locations of the EEG channels used in the CAR spatial filtering circuit of the smart EEG cap were distributed over large region of the brain hemisphere to successfully avoid the above issue. Finally, the performance of the proposed smart EEG cap on motion imagery detection was also tested. The averaged accuracy of the proposed smart EEG cap on motion-imagery detection was $73.19 \pm 5.20\%$, and the ITR was about 1.01 bits per trial.

In previous studies, several online motion imagery-based BMIs with or without the function of selecting channels have been successfully proposed [17–19]. System comparison between proposed system and other online motion-imagery BMIs is shown in Table 1. In 2015, Ang et al. implemented an online motion imagery BMI to assist neurorehabilitation for stroke patients [20]. Here, 27 EEG channels were used, and filter bank common spatial pattern (FBCSP) algorithm was used to construct a patient-specific model from a calibration session to recognize motion imagery. Its accuracy was about 70%. In 2016, Handiru et al. proposed the approach of the iterative multi-objective optimization for channel selection (IMOCS) to find a set of the most relevant channels [21], and applied it in the design of the motion-imagery BMI. Here, 16 or 20 channels would be selected by the IMOCS method from 64 EEG channels, and its averaged accuracy was about 63%. In 2018, Cantillo-Negrete et al. also designed an online motion imagery BMI to control a robotic hand orthosis [22]. Here, a bank of temporal filters and the common spatial pattern algorithm were used for feature extraction and the particle swarm optimization was used for feature selection. Eleven electrodes (F3, F4, Fz, C3, C4, Cz, T3, T4, P3, P4, and Pz in the international 10–20 EEG system) were placed over the scalp of the participants. It online performance was about 70%. In this study, by using the proposed smart EEG cap, the performance of the motion imagery BMI was similar to the above online motion imagery-based BMIs. However, the above online motion imagery-based BMIs still have to transmit multi-channel brain responses to a computer to execute the function of selecting channels and detecting motion imagery. Different from other BMIs, the front-end smart EEG cap could perform the function of selecting channels directly, and only the selected-channel EEG signals would be sent to the back-end computer to reduce the loading of transmission data and computation complexity. Moreover, the advantages of measuring EEG without conductive gels and wireless transmission also greatly improved the practicability of BMI applications in daily life. In the future, both of the feature selection and classification procedure can be integrated into the smart cap.

6. Conclusions

In this study, a smart EEG cap was proposed to select the relevant EEG channels and enhance EEG features within a local spatial distribution. Here, dry active electrodes with spring loaded were also implemented and applied in the smart EEG cap, to measure brain responses without conductive gels, in the hairy head skin. Moreover, by using the design of the common average reference spatial filtering circuit, the front-end smart EEG cap could directly execute the function of spatial filtering, and its performance of enhancing ERD feature was about 17.33%. Different from other EEG machines used in previous BMIs, the proposed smart EEG cap could perform the function of selecting channel in the front-end EEG cap to only transmit the selected-channel EEG signals. Finally, the proposed smart EEG cap was also applied in

Table 1
System comparison between proposed system and other online motion-imagery BMIs.

	Ang et al. [20]	Handiru et al. [21]	Cantillo-Negrete et al. [22]	Proposed system
Number of used EEG channels	27	64	11	8
Type of EEG electrode	Conventional EEG electrode	Conventional EEG electrode	Conventional EEG electrode	Dry active electrode
Accuracy (%)	70	63	70	73.19
Bit rate (bits/min)	–	–	–	6.06
Function of selecting channel	No	Yes	No	Yes
Unit of computing ERD	Back-end computer	Back-end computer	Back-end computer	Front-end smart EEG cap
Wearability	No	No	No	Yes
Wireless module	No	No	No	Bluetooth module

the design of the motion-imagery BMI. The experimental results showed that the proposed smart EEG cap exactly provided a good performance of detecting motion imagery (the averaged accuracy was $73.19 \pm 5.20\%$, and the ITR was about 6.06 bits/min). The advantages of the proposed smart EEG cap on measuring EEG without conductive gels and wireless transmission could effectively improve the convenience of use, and reduce the limitation of activity in daily life. Therefore, the proposed smart EEG cap is a system prototype of a novel wearable EEG device, and in the future, it might be widely applied in other BMI applications.

Declaration of Competing Interest

The authors declare no conflict of interest.

Acknowledgments

This research was partly supported by Ministry of Science and Technology in Taiwan, under grants MOST 107-2221-E-009-017 and MOST 107-2221-E-305-014. This research was also partly supported by University System of Taipei Joint Research Program, under grants USTP-NTPU-TMU-107-02, and Faculty Group Research Funding Sponsorship by National Taipei University, under grants 2018-NTPU-ORDA-04. This work was also supported by the Higher Education Sprout Project of the National Chiao Tung University and Ministry of Education (MOE), Taiwan. Asterisk indicates corresponding author.

Supplementary materials

Supplementary material associated with this article can be found, in the online version, at doi:10.1016/j.cmpb.2019.06.009.

References

[1] G.S. Mason, E.G. Birch, A general framework for brain–computer interface design, IEEE Trans. Neural. Syst. Rehabil. Eng. 11 (1) (2003) 70–85.
[2] G. Pfurtscheller, F.H. Lopes da Silva, Event-related EEG/MEG synchronization and desynchronization: basic principles, Clin. Neurophysiol. 110 (11) (1999) 1842–1857.
[3] M. Arvaneh, C. Guan, K.K. Ang, C. Quek, Optimizing the channel selection and classification accuracy in EEG-based BCI, IEEE Trans. Biomed. Eng. 58 (6) (2011) 1865–1873.
[4] T. Lal, M. Schroder, T. Hinterberger, J. Weston, M. Bogdan, N. Birbaumer, B. Schölkopf, Support vector channel selection in BCI, IEEE Trans. Biomed. Eng. 51 (6) (2004) 1003–1010.
[5] T. Lan, D. Erdogmus, A. Adami, S. Mathan, M. Pavel, Channel selection and feature projection for cognitive load estimation using ambulatory EEG, Comput. Intell. Neurosci. 8 (2007) 8–20.
[6] T.C. Ferree, P. Luu, G.S. Russell, D.M. Tucker, Scalp electrode impedance, infection risk, and EEG data quality, Clin. Neurophysiol 112 (3) (2001) 536–544.
[7] D.J. McFarland, L.M. McCane, S.V. David, J.R. Wolpaw, Spatial filter selection for EEG-based communication, Electroencephalogr. Clin. Neurophysiol. 103 (3) (1997) 386–394.
[8] G. Pfurtscheller, A. Aranibar, Evaluation of event-related desynchronization (ERD) preceding and following voluntary self-paced movement, Electroencephalogr. Clin. Neurophysiol. 46 (2) (1979) 138–146.
[9] G. Pfurtscheller, A. Stancák, Ch. Neuper Jr., Event-related synchronization (ERS) in the alpha band–an electrophysiological correlate of cortical idling: a review, Int. J. Psychophysiol. 24 (1–2) (1996) 39–46.
[10] G. Pfurtscheller, Functional brain imaging based on ERD/ERS, Vision Res. 41 (2001) 1257–1260.
[11] B.-S. Lin, B.-S. Lin, F.-C. Chong, Feipei Lai, Higher-order-statistics-based radial basis function networks for signal enhancement, IEEE Trans. Neural Netw. 18 (3) (2007) 823–832.
[12] J.R. Wolpaw, H. Ramoser, D.J. McFarland, G. Pfurtscheller, EEG-based communication: improved accuracy by response verification, IEEE Trans. Rehabil. Eng. 6 (3) (1998) 326–333.
[13] J.R. Pierce, An Introduction to Information Theory: Symbols, Signals and Noise, Dover, New York, 1980.
[14] Y.J. Huang, C.Y. Wu, A.M.K. Wong, B.S. Lin, Novel active comb-shaped dry electrode for EEG measurement in hairy site, IEEE Trans. Biomed. Eng. 62 (1) (2015) 256–263.
[15] M.J. Alhaddad, Common average reference (CAR) improves P300 speller, Int. J. Eng. Technol. 2 (2012) 451–456.
[16] S.C. Ng, P. Raveendran, Comparison of different montages on to EEG classification, in: IFMBE Proceedings of the 3rd Kuala Lumpur International Conference on Biomedical Engineering, 15, Kuala Lumpur, Malaysia, 2006, pp. 365–368. 11–14.
[17] Y. Jiao, Y. Zhang, X. Chen, E. Yin, J. Jin, X. Wang, A. Cichocki, Sparse group representation model for motor imagery EEG classification, IEEE J. Biomed. Health Inform. 23 (2) (2019) 631–641.
[18] Y. Zhang, C.S. Nam, G. Zhou, J. Jin, X. Wang, A. Cichocki, Temporally constrained sparse group spatial patterns for motor imagery BCI, IEEE Trans. Cybern. 99 (2018) 1–11.
[19] Y. Zhang, G. Zhou, J. Jin, X. Wang, A. Cichocki, Optimizing spatial patterns with sparse filter bands for motor-imagery based brain–computer interface, J, Neurosci. Methods 255 (2015) 85–91.
[20] K.K. Ang, C. Guan, Brain–computer interface for neurorehabilitation of upper limb after stroke, Proc. IEEE 103 (2015) 944–953.
[21] V.S. Handiru, V.A. Prasad, Optimized bi-objective EEG channel selection and cross-subject generalization with brain–computer interfaces, IEEE Trans. Hum–Mach Syst. 46 (6) (2016) 777–786.
[22] J. Cantillo-Negrete, R.I. Carino-Escobar, P. Carrillo-Mora, D. Elias-Vinas, J. Gutierrez-Martinez, Motor imagery-based brain-computer interface coupled to a robotic hand orthosis aimed for neurorehabilitation of stroke patients, J. Healthc. Eng. 2018 (2018) 1–10 Article 1624637 (2018).